

BRANDENBURGISCHE TECHNISCHE
UNIVERSITÄT COTTBUS-SENFTEMBERG

LAVAL NOZZLE

14040 | COMPUTATIONAL FLUID DYNAMICS FOR ENGINEERS

AUTHORS

MAHEK ATUL SANGHVI

Student No. 5006589

SUPERVISOR

DR. PETER SZABO

COTTBUS, FEBRUARY 2024

Declaration

In accordance with the appropriate regulations, I hereby submit my project and I declare that:

- the report embodies the results of my own work and has been composed by myself
- where appropriate, I have made acknowledgement of the work of others and have made reference to work carried out in collaboration with other persons
- the report is the correct version of the report for submission and is the same version as any electronic versions submitted*.
- I understand that as a student of the University I am required to abide by the Regulations of the University and to conform to its discipline.
- I confirm that the report has been verified against plagiarism via an approved plagiarism detection application e.g. Turnitin.
- I declare that the lecturer can submit the electronic copy of the report to a plagiarism detection application e.g. Turnitin.
- I have not used any AI tools or technologies to prepare this assessment.

* Please note that it is the responsibility of the student to ensure that the correct version of the report is submitted.

Name of student _____

Date: _____

Signature of Student: _____

ABSTRACT

The Laval nozzle is one of the important factors for engines to get exit Mach numbers greater than 1 or supersonic flows. Engines generally have restrictions with combustion zones as many factors hold them from supplying high amounts of energy such as temperature, materials, and many more. This leads to the need for a nozzle that converts the pressure energy into velocity and further, the shape governs the flow to increase its velocity and provide a Mach number above 1.

This project focuses on flow inside a Laval nozzle by CFD using Open FOAM software. The Laval nozzle is pressure driven in this case and pressure is provided at both ends and varying the pressure at exit, variation of flow is observed. Now to achieve supersonic flows there is a hurdle known as shocks. During this simulation shock can be observed and the way it moves forward through the diverging part of the nozzle and finally we achieve supersonic flows.

This project aims to analyse the flow inside a nozzle and find the optimum point for which inlet pressure could be observed by the combustion zone to reach ambient pressure in real life for optimum expansion from subsonic flow to supersonic flows.

Keywords: Laval nozzle, Supersonic flow, Shock

CONTENTS

Contents	iii
List of Figures	v
List of Tables	vi
1 Introduction	1
2 Methodology	2
2.1 Model Formation	2
2.1.1 Objective	2
2.1.2 Theoretical Background	2
2.1.3 Governing Equations	4
2.1.4 Boundary Conditions & Initial Conditions	4
2.1.5 Analytical Calculations	5
2.2 Computational Methodology	6
2.2.1 Geometry	6
2.2.2 Mesh	7
2.2.3 Constants	7
2.2.4 Discretization Schemes	8
2.2.5 Solver	8
3 Results	10
3.1 Mesh Convergence & Bench marking	10
3.2 Results & Discussion	10
3.2.1 Subsonic case	11
3.2.2 Supersonic case with shocks	11
3.2.3 Supersonic case	15
3.2.4 Pressure variation	16
3.2.5 Final Discussion	17
4 Conclusion	18
4.1 Limitations	18
5 References	19
Appendices	
A Appendix A	21
A.1 BlockMeshDict	21
A.2 Pressure	24
A.3 Temperature	25
A.4 Velocity	26
A.5 FVSolution	27
A.6 FVSchemes	28
A.7 ControlDict	30

A.8 Turbulence Properties	32
A.9 Thermal Properties	33

LIST OF FIGURES

2.1	Entire geometry of Laval nozzle having an inlet domain with dimensions used for simulation	6
2.2	Mesh generated for the geometry of Laval nozzle and its domain	7
3.1	Plot of Mach number against the diverging section of the nozzle for course, medium and fine mesh and also comparison with analytical results	11
3.2	Mach number contour for Laval nozzle for subsonic case at an outlet pressure of 9371 Pa	12
3.3	Pressure contour for Laval nozzle for subsonic case at an outlet pressure of 9371 Pa	12
3.4	Mach number contour for Laval nozzle for supersonic case with a standing normal shock wave at an outlet pressure of 5280 Pa	13
3.5	Pressure contour for Laval nozzle for supersonic case with a standing normal shock wave at an outlet pressure of 5280 Pa	13
3.6	Density contour for Laval nozzle for supersonic case with a standing normal shock wave at an outlet pressure of 5280 Pa	14
3.7	Temperature contour for Laval nozzle for supersonic case with a standing normal shock wave at an outlet pressure of 5280 Pa	14
3.8	Mach number contour for Laval nozzle for supersonic case without shocks at an outlet pressure of 939 Pa	15
3.9	Pressure contour for Laval nozzle for supersonic case without shocks at an outlet pressure of 939 Pa	15
3.10	Plot depicting the changes in mach number, area ratio, velocity, temperature, and density along the pressure ratio of the Laval nozzle in a supersonic scenario without the presence of any shocks.	16
3.11	Plot of pressure ratio along the nozzle length non-dimensionlized for outlet pressures of 939Pa (supersonic), 5280Pa, 6000Pa, 7250Pa, 8500Pa, 9371Pa for the Laval nozzle	17

LIST OF TABLES

2.1	Boundary conditions of Laval nozzle flow for pressure, velocity and temperature	5
2.2	Mach number, Pressure ratio and exit pressure calculations analytically solved for a fixed area ratio	6
2.3	Constants of the mixture properties of the fluid with their values	7
2.4	Assumed thermal properties of the fluid	8
3.1	Comparison of data with different mesh size and also comparison with analytical data	10
3.2	Pressure variation cases for different outlet pressures and corresponding exit mach number observed with comments	16
3.3	Comparison of results for exit Mach number with analytical results for subsonic, normal shock, and supersonic cases with error in %	17

INTRODUCTION

Laval nozzle is a type of nozzle mainly used in industries where subsonic speed is used to convert to supersonic speed, mainly in rocket engines and supersonic missiles. Laval nozzle is used in rocket engines where for the generated combustion a speed greater than Mach 1 is required to leave the earth's surface's gravity or even for higher speeds where a specific time is required by the satellite to reach a position for it to work in a specific time. Just by increasing combustion will only lead to an increase in temperature but the conversion of that energy is the most important phenomenon to be studied which is possible in the Laval Nozzle.

The Laval nozzle generally has three parts in its geometry. Firstly, it has a converging part where the subsonic speed having a large amount of pressure is converted to velocity and flow at the second region which is the throat has a velocity higher than the subsonic speed. To get a supersonic speed the throat should have a Mach number up to 1 which is the sonic speed to get an output of higher than sonic speed. The third part is the diverging section where due to Mach greater than 1 the diverging part acts as a nozzle as well due to which velocity is increased and in turn, the Mach goes above 1 making it supersonic speed.

The major reason for the Laval nozzle is to convert subsonic flow to supersonic flow but there is a biggest problem which is shocks. Shocks are nothing but abrupt changes in flow characteristics which are there in the diverging section of the Laval nozzle and are used to increase velocity but due to shocks there is a very big drop in velocities and high pressure rise which is a big challenge to focus on.

METHODOLOGY

2.1 Model Formation

2.1.1 Objective

Conducting research through computational means for investigating a pressure-driven Laval nozzle. The study is focused on varying the pressure to observe the flow and to solve for cases which lead to the formation of shocks and variations it provides in physical quantities like pressure, mach number, temperature and density. The major investigation is to achieve supersonic flow at nozzle exit with subsonic flow at nozzle inlet which is the major objective of the Laval nozzle.

2.1.2 Theoretical Background

Mach Number

Mach number is a dimensionless number defined as the ratio of the speed of a body to the speed of sound. Equation 2.1 describes the definition of the Mach number.

$$M = \frac{u}{c} \quad (2.1)$$

Where:

M – Mach Number

u – speed of the object in m/s

c – speed of sound in m/s

Area Velocity Relation

Area changes are possible in 2 ways either in converging part and diverging part, due to which the behavior of flow changes. If the flow velocity increases and pressure decreases, then it is referred to as a nozzle. If velocity decreases and pressure increases, then it is referred to as a diffuser. The understanding of the flow behaving as a nozzle or diffuser is determined by the famous area velocity relation as mentioned in Equation 2.2. At subsonic speed, the increase in area works as a diffuser, and decrease in area acts as a nozzle. It is vice versa in the case of supersonic speeds.

$$\frac{dA}{A} = \frac{dv}{v} (M^2 - 1) \quad (2.2)$$

Where:

A – cross-sectional area in m^2
 v – flow velocity in m/s
 M – Mach Number

Area Mach Rule

Equation 2.3 describes that for a given area ratio, which is the ratio of exit area to throat area, there are 2 possible solutions for exit Mach number in which one will lie in the subsonic case and the other in the supersonic case. This mainly depends on the pressure ratio, which is the ratio of pressure at inlet to pressure at exit.

$$\frac{A}{A^*} = \left(\frac{1}{M} \right) \left[\frac{2}{\gamma + 1} \left(1 + \frac{\gamma - 1}{2} M^2 \right) \right]^{\frac{\gamma + 1}{2(\gamma - 1)}} \quad (2.3)$$

Where:

A – cross-section of exit in m^2
 A^* – cross-section of throat in m^2
 M – exit Mach number
 γ – specific heat ratio

Isentropic Relations

Isentropic relations are used in cases of flows where one parameter is known and another parameter could be found out, either at the same location or at another location only if it is an adiabatic case. In Equation 2.4 represents the ratio of pressure as a function of exit mach number.

$$\frac{P}{P_e} = \left(\frac{T}{T_e} \right)^{\frac{\gamma}{(\gamma - 1)}} = \left(1 + \frac{\gamma - 1}{2} M_e^2 \right)^{\frac{-\gamma}{(\gamma - 1)}} \quad (2.4)$$

Where:

P, P_e – Pressure at inlet & exit respectively in Pa
 T, T_e – Temperature at inlet & exit respectively in K
 M_e – Mach number at exit

Normal Shock Relations

Normal shocks are sudden jumps or discontinuity which is not easily determined at what location or what changes it can bring due to which Equation 2.5 is used to find the pressure jump downstream of the pressure and Equation 2.6 is used to find the mach number loss for downstream of the shock.

Pressure Ratio:

$$\frac{p_2}{P_1} = \frac{1 + \frac{\gamma - 1}{2} M_1^2}{\gamma M_1^2 - \frac{\gamma - 1}{2}} \quad (2.5)$$

Where:

P_2 – Pressure upstream of shock in Pa
 P_1 – Pressure downstream of shock in Pa
 M_1 – Mach number upstream of shock

Mach Number:

$$M_2 = \sqrt{\frac{M_1^2 + \frac{2}{\gamma-1}}{\frac{2\gamma}{\gamma-1}M_1^2 - 1}} \quad (2.6)$$

Where:

M_1 – Mach number upstream of shock
 M_2 – Mach number downstream of shock

2.1.3 Governing Equations

During simulating such a complex phenomenon governing equations are integral part which needs to be formulated based on few assumptions made listed below:

1. Compressible flow
2. Laminar flow
3. In-viscid flow
4. Gravitational effects are neglected
5. Steady flow

Based on our assumptions "rhoCentralFoam" solver was employed available in Open FOAM for solving compressible flows and other assumptions were developed in the code part of this solver. The solver rhoCentralFoam is a density-based solver which is unlike the usual solvers like rhoSimpleFoam and rhoPimpleFoam which can also be used for compressible flows but they are pressure-based solvers. rhoCentralFoam is a transient solver and highly unstable and employs central upwind schemes formulated by Kurganov and Tadmor.

The governing equations are based on the solver and various assumptions made they are formulated for the conservation of mass in Equation 2.7 and conservation of momentum in Equation 2.8.

Continuity Equation

$$\nabla \cdot (\mathbf{U}\rho) = 0 \quad (2.7)$$

Momentum Equation (Navier-Stokes)

$$\nabla \cdot (\rho \mathbf{U}\mathbf{U}) + \nabla p = 0 \quad (2.8)$$

Where,

ρ is the density in kg/m³,

\mathbf{U} is the velocity vector in m/s,

p is the pressure in Pa,

Based on the assumptions the Equation 2.8 momentum is re framed as Equation 2.9

$$u \frac{du}{dx} = -\frac{c^2}{\rho} \frac{d\rho}{dx} \quad (2.9)$$

And finally substituting this in general Bernoulli's equation we get an equation which same as area velocity relation as in Equation 2.2 which is the area velocity relation.

2.1.4 Boundary Conditions & Initial Conditions

The entire geometry is divided into different boundaries and has been assigned the following boundary or initial conditions based on the Laval nozzle working. The left end is named the inlet, the top plane and the nozzle are named as wall, the symmetrical axis is named as symmetry plane and the nozzle exit is named as outlet. Different types of boundary and initial conditions are mentioned below.

Boundary	P	U	T
Inlet	totalPressure	zeroGradient	fixedValue
Outlet	fixedValue	zeroGradient	zeroGradient
Wall	zeroGradient	slip	zeroGradient
Bottom	symmetryPlane	symmetryPlane	symmetryPlane
Top	zeroGradient	slip	slip

Table 2.1: Boundary conditions of Laval nozzle flow for pressure, velocity and temperature

Inlet

The inlet is given as a boundary with initial conditions of total pressure which is a Dirichlet boundary condition as it explicitly sets the inlet as total pressure. The inlet pressure is kept as 10000 Pa and remained fixed throughout the simulation.

Outlet

The outlet is given as a boundary with initial conditions of fixed value which is a Dirichlet boundary condition and the pressure is a fixed value. As we study different cases of a pressure-driven Laval nozzle we change the values of pressure for observing the pressure variations throughout the nozzle. Only for a single case the outlet is kept as wavetransmissive to observe supersonic flows since fixed-value cannot be kept since the outlet of nozzle needs to be extended since shocks travel further after a point.

Symmetry plane

The mid-axis of the nozzle is considered symmetrical due to geometry and also for simulation purposes, it can be assumed since we are observing laminar flow. In this boundary condition, the properties are mirrored across the symmetrical plane. It is a special case of the Dirichlet boundary condition.

Wall

The wall represents the nozzle wall and the top plane of the domain which is given as the boundary condition with zero-gradient which shows that the gradient to the wall for pressure and temperature is zero-gradient but for velocity, it is a slip condition since assuming that there is no friction between the wall and the flow. This is a Neumann boundary condition since we mention the gradient of a property and not directly the property such as pressure, temperature and velocity.

The boundary conditions for pressure driven Laval nozzle have been tabulated in Table 2.1.

2.1.5 Analytical Calculations

To perform the analysis and to confirm the results analytical calculations is important. The area ratio which is the ratio exit area to inlet area of nozzle is kept at a constant 2x in our case. Using this known value Equation 2.3 is used to calculate the exit mach number. As the equation holds a square term due to which 2 solutions are found and they are tabulated in Table 2.2. One will be observed in subsonic range and one in supersonic range. During the simulation both is achieved since using this exit mach number we also calculate the pressure ratio for both cases using the Equation 2.4. This is an isentropic equation which is used to find the pressure ratio from the exit mach number.

Case	Subsonic	Supersonic
Area Ratio ($A_{\text{exit}}/A_{\text{throat}}$)	2	2
Mach Number	0.3059	2.1972
Pressure Ratio ($P_{\text{exit}}/P_{\text{inlet}}$)	0.9371	0.0939
Exit Pressure	9371	939

Table 2.2: Mach number, Pressure ratio and exit pressure calculations analytically solved for a fixed area ratio

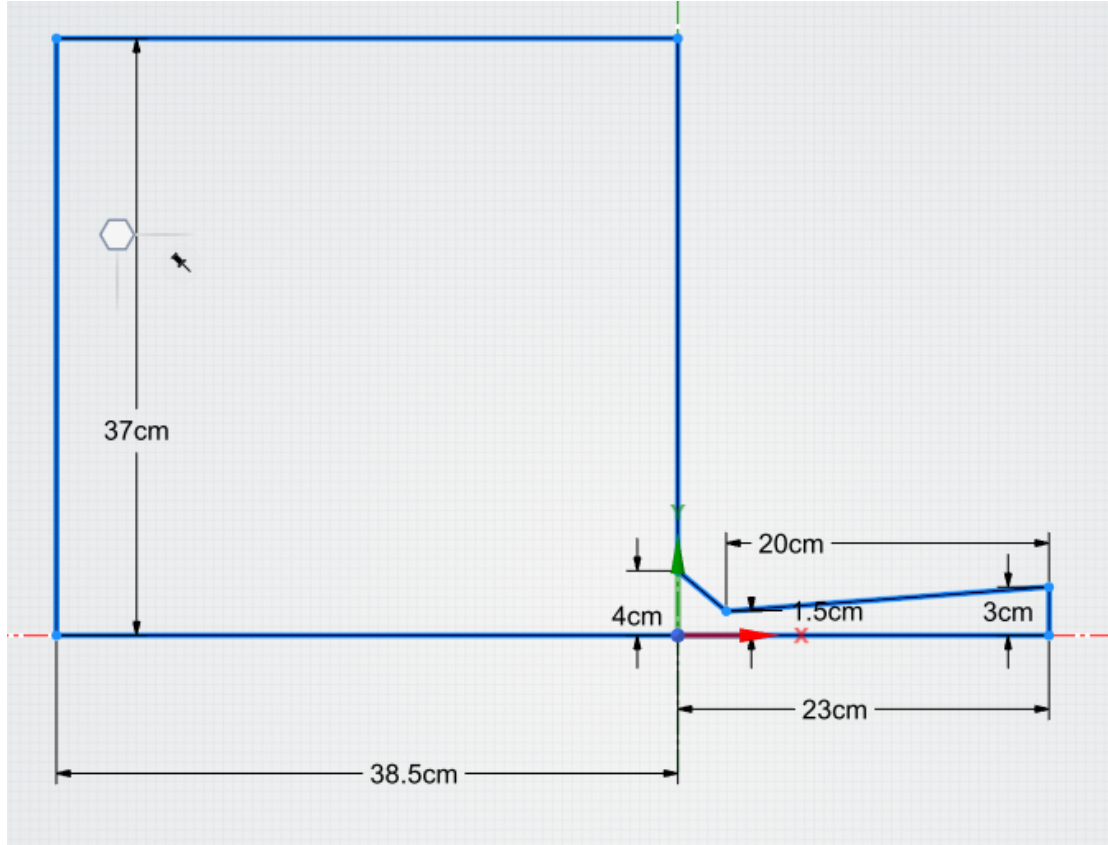


Figure 2.1: Entire geometry of Laval nozzle having an inlet domain with dimensions used for simulation

2.2 Computational Methodology

2.2.1 Geometry

The general construction of a nozzle is done with a converging and diverging part and it was constructed with an area ratio to be 2 for better and easier calculations analytically. The general construction of geometry is studied [3]. The blockMeshDict file in Appendix A.1 is used to construct the geometry of the nozzle. Also additionally an ambient domain is created for the flow parameters to be initialized. The entire geometry created is symmetrical so only half of the nozzle is created to save computation time. Figure 2.1 represents the geometry of the nozzle with dimensions.

The geometry is defined by the function given in the Equation 2.10 and in Equation 2.11.

$$y = 0.667 \cdot x + 0.04, \quad \text{if } -0.03 \leq x \leq 0 \quad (2.10)$$

$$y = 0.75 \cdot x + 0.015, \quad \text{if } 0 \leq x \leq 0.2 \quad (2.11)$$

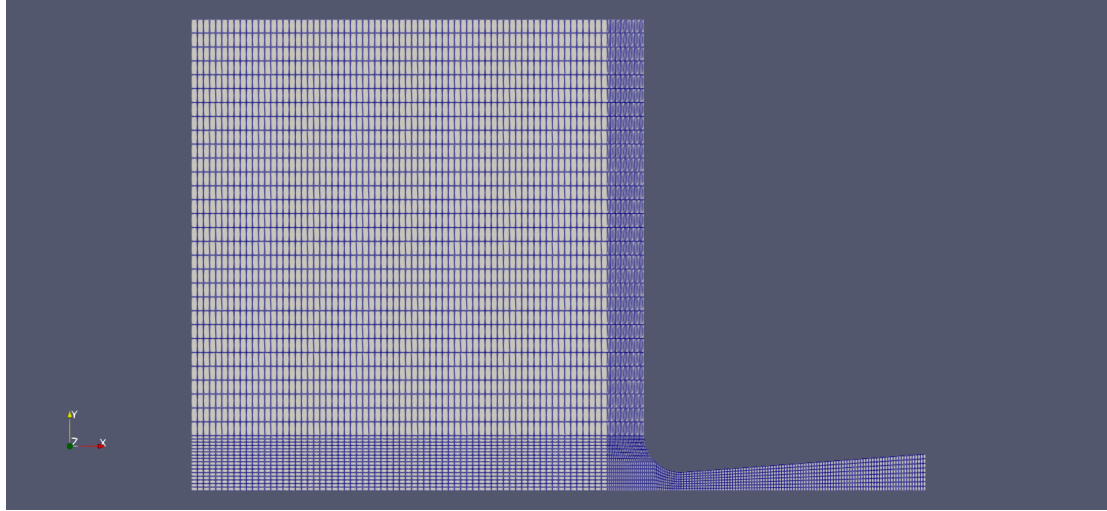


Figure 2.2: Mesh generated for the geometry of Laval nozzle and its domain

Constants	Values
Number of moles	1
Molecular weight	29
Coefficient of Pressure	1005
Viscosity	0
Prandtl Number	1

Table 2.3: Constants of the mixture properties of the fluid with their values

2.2.2 Mesh

The geometry is subdivided into 8 sections for finer meshing and the mesh is made denser at the entrance of the nozzle and also inside the nozzle but the outside domain is kept constant. The meshing done is through hex mesh in blockMeshDict which has three-dimensional cells with six faces and each face is quadrilateral. Also, simple grading is employed as a unit in all directions for simpler meshing. The mesh properties are described below:

- points = 10484
- faces = 20247
- hexahedral cells = 5002
- Max cell openness = 2.13363e-16
- Max aspect ratio = 8.68889
- Minimum face area = 1.30435e-06
- Maximum face area = 5.66667e-05
- Min volume = 3.34443e-09
- Max volume = 5.66667e-08
- Mesh non-orthogonality Max: 41.0153 average: 3.84201
- Max skewness = 1.00739

The Figure 2.2 represents the meshing done on the entire geometry with the above properties. It is clearly visible that mesh is coarser near the domain and it keeps on getting finer as it moves towards the nozzle.

2.2.3 Constants

During the simulation there is a need to create some constants and assumptions of flow for thermal properties. The list of constants for the mixture of fluid and flow assumptions have been tabulated in the Table 2.3 and Table 2.4 respectively for thermal properties.

Property	Assumed
Type	hePsiThermo
Mixture	Pure
Transport	constant
Thermo	Enthalpy Constant
Equation of state	Perfect Gas

Table 2.4: Assumed thermal properties of the fluid

2.2.4 Discretization Schemes

To solve for the various parameters like pressure, velocity and temperature it is important to provide mathematical ways for the solver to solve the equations based on many factors like, computation time, accuracy, mesh and methodology of the solve. Combination of all these factors the decision of different schemes is made. These schemes help to solve the equations in spatial and temporal derivative.

Understanding many factors like:

- The solver which highly unstable and is transient and time dependent solver .
- The computation power of the PC.
- Accuracy to be minimal for this case.
- Mesh of the domain is quite uneven.

Based on the following assumptions the following discretization schemes are used.

- Divergence Schemes: Gauss linear (linear interpolation for spatial gradients)
- DDt Schemes: Euler (First order explicitly solved time integration)
- Laplacian Schemes: Gauss linear corrected (corrected linear scheme)
- Interpolation Schemes: default linear and for pressure, velocity and temperature vanAlbada schemes.
- snGrad Schemes: corrected (calculating gradient of surface normal's).

2.2.5 Solver

The solver used in this project is rhoCentralFoam which is a density-based solver. Since Open FOAM uses a finite volume approach the governing equations are integrated.

The first step of the solver is an iterative process for important parameters like density and velocity along the time loop. Later the calculations of pressure are performed with the help of Equation 2.12.

$$p = \frac{\rho}{Z} \quad (2.12)$$

where,

Z is the compressible factor.

ρ is the density in kg/m^3

Steps to solve the governing equations

1. Solving for conservation of mass equations:

To solve the mass equation it solves for density-weighted fields. Hence the first step is to interpolate the parameters in directions of x and y both.

The next step involves a calculation of the speed of sound by the solver which is the parameter to be known since interest lies in Mach number. And later their volumetric fluxes are calculated.

Now the weightings and diffusive part are calculated using the central upwind scheme formulated by Kurganov as observed in Equation 2.13 and Equation 2.14.

$$\alpha = \frac{\phi_f}{\phi_{f+} - \phi_{f-}} \quad (2.13)$$

$$\omega_f = -\alpha (1 - \alpha) (\phi_{f+} - \phi_{f-}) \quad (2.14)$$

Where,

α is calculated on the ϕ_f which represents for a face f .

ϕ_{f+} and ϕ_{f-} are the parameters on the right and left of the face.

After all these iterations the solver solves for density from the mass conservation equation.

2. Solving for momentum equations:

The Momentum equations are solved in 2 steps. Since we consider in-viscid flows the energy equations are not solved but the momentum is solved and it has diffusive parameters from velocity and temperature.

Implicitly the in-viscid momentum equations are solved and velocity is updated. And hence the momentum equations are solved for coupling of pressure and velocity.

In this case the fvsolvers used for density is diagonal solver which is used in cases where solving the parameters is mostly a diagonal matrix. In case of velocity the smooth solver is used and has been set for Gauss Seidal with tolerance to 1e-09. And same properties are inherited to energy as solver for the velocity with tolerance limit as 1e-10.

RESULTS

3.1 Mesh Convergence & Bench marking

Mesh convergence is done to study the properties change as we change the mesh size and cells. To know this we compare this results with different mesh sizes and as the cells increase the change in properties do not vary much and then we finalize the mesh and do the further study using that mesh. Also mesh convergence is done for the case of most drastic case in this condition it is the production of shocks. Hence a case of shock is taken and mesh convergence is performed.

Figure 3.1 shows the plot of Mach number along the diverging section of the nozzle. The mesh convergence is combined with bench marking as we also compare the results with analytical calculation using the area mach relations as in Equation 2.3.

During mesh convergence the number of cells, mach number before shock and mach number after shock and location of shock are tabulated in table 2.2 and based on that we conclude to use medium mesh to get a closer results.

And finalization of medium mesh is done because it reduces computation time and results are much closer and do not hinder as fine mesh which could be because of solver used. Also observing the results compared with analytical results error is very less in the end result. This clearly indicates the use of medium mesh to perform further analysis for pressure variation and supersonic flows.

3.2 Results & Discussion

Simulation is performed for different cases where the inlet pressure is kept constant and changes have been made to outlet pressure. During the process of varying the pressure there are mainly three cases are formed for this geometry. Each case is discussed with the contour and finally the pressure variations and the case where supersonic case is achieved and discussed in much detail in 3.2.3.

During the simulation the outlet pressure is 10000Pa and outlet pressure is varied to 9371 Pa, 8500 Pa, 7250 Pa, 6000Pa and 5280 Pa. The variation of each case is discussed in 3.2.4.

Mesh Type	No. of Cells	Mach before shock	Mach after shock	Shock location
Course	510	2.1	0.58	1.86
Medium	2050	2.14	0.55	1.92
Fine	8200	2.16	0.53	1.94
Analytical results	-	2.17	0.54	1.96

Table 3.1: Comparison of data with different mesh size and also comparison with analytical data

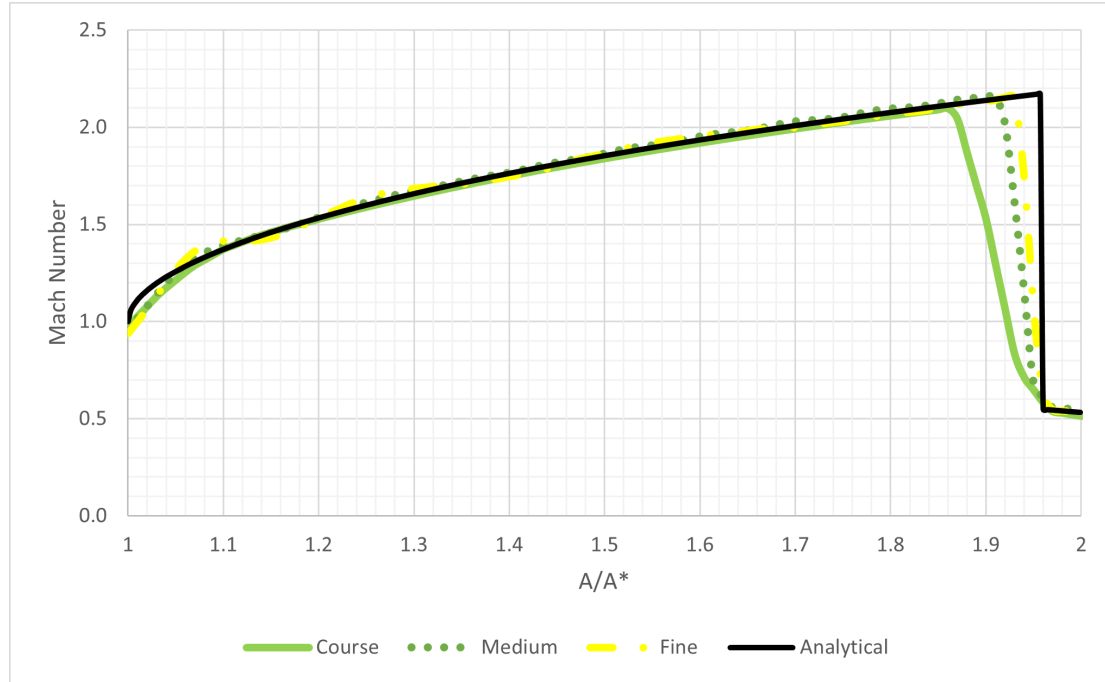


Figure 3.1: Plot of Mach number against the diverging section of the nozzle for course, medium and fine mesh and also comparison with analytical results

3.2.1 Subsonic case

Laval nozzle is mainly used to achieve an exit mach number greater than 1 but if the pressure variation is quite low then the exit mach remains in subsonic itself. In this case the outlet pressure was kept as 9371 Pa.

The Figure 3.2 and Figure 3.3 shows the variation of mach number and pressure respectively. It is observed that the mach firstly increases and upto the throat and then it decreases back. This is because during the flow at the inlet it has converging section so it acts as a nozzle and while it reaches throat the flow is still not reached a case where flow is either unity or greater than 1 due to which the the diverging part instead of acting as nozzle it acts as a diffuser due to which flow decelerates and mach number again reduces.

3.2.2 Supersonic case with shocks

The Laval nozzle is now set to higher pressure difference to reach the case of supersonic case since with lower pressure difference this was not possible. During increasing the pressure difference the flow now should reach a supersonic case but there is friction to perform this since the flow has mach number above 1 the flow properties flow faster than speed of sound. During this process the flow particles when colliding to increase the speed are unable to provide the information to further particles due to which all particles collide and form a shock.

In this case the pressure is kept as 5280 Pa. In Figure 3.4 which is contour plot of mach where the flow mach number increase from inlet to the nozzle as converging part acts as a nozzle and also at throat the flow is towards little greater than unity due to which flow now is supersonic according to the flow due to which the diverging part acts as nozzle again and flow is turned into supersonic but there is a shock before the flow exits the nozzle and due to this mach number drops. It could also be observed in Figure 3.5 that the pressure is very high after the shock because of sudden stoppage of flow. Also in Figure 3.6 the density iso contour the flow has drastically increased and this is because of consideration of compressible flows. In Figure 3.7 we could observe also there is sudden increase in temperature downstream of the shock.

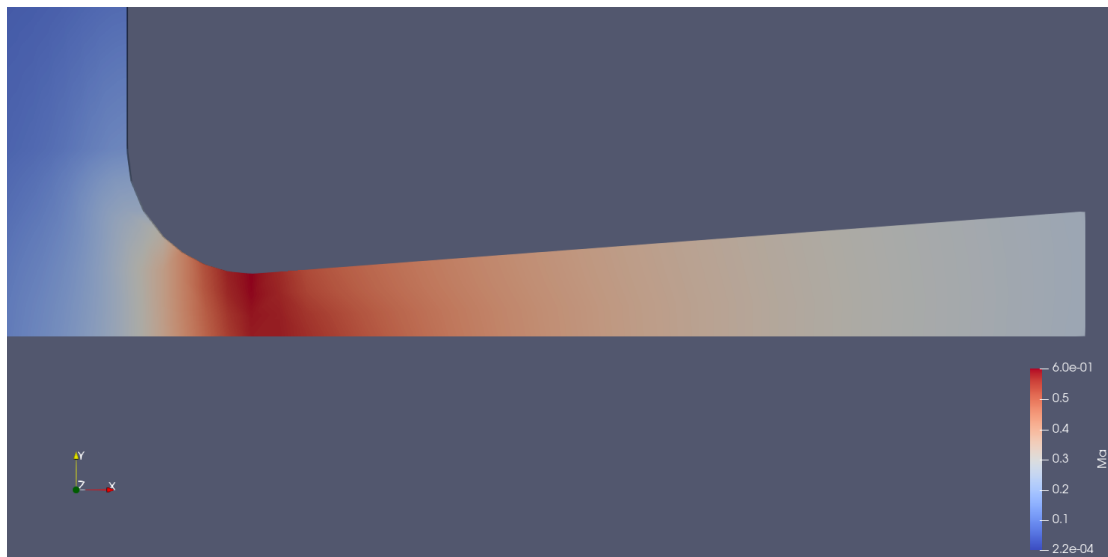


Figure 3.2: Mach number contour for Laval nozzle for subsonic case at an outlet pressure of 9371 Pa

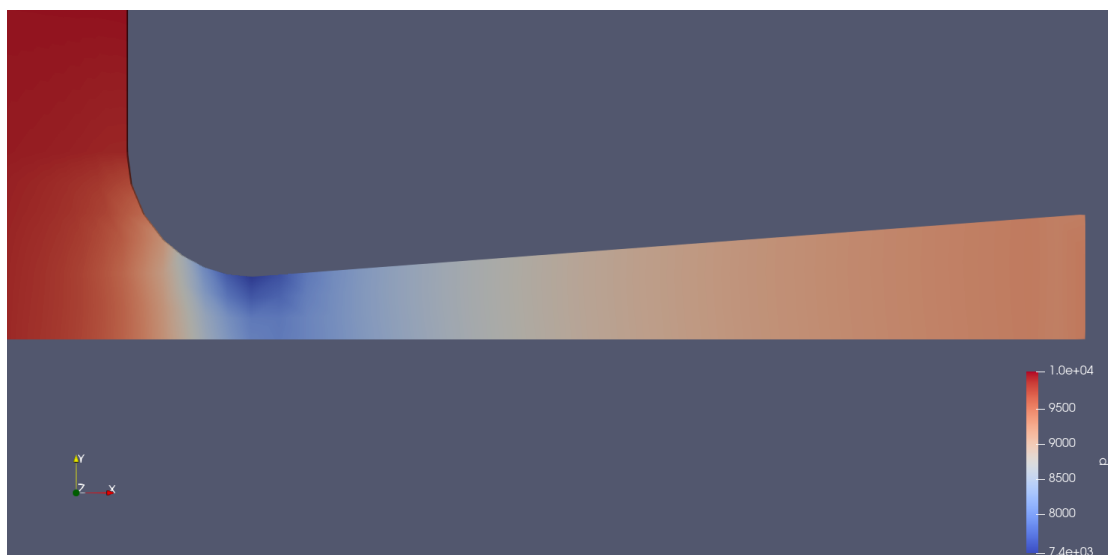


Figure 3.3: Pressure contour for Laval nozzle for subsonic case at an outlet pressure of 9371 Pa

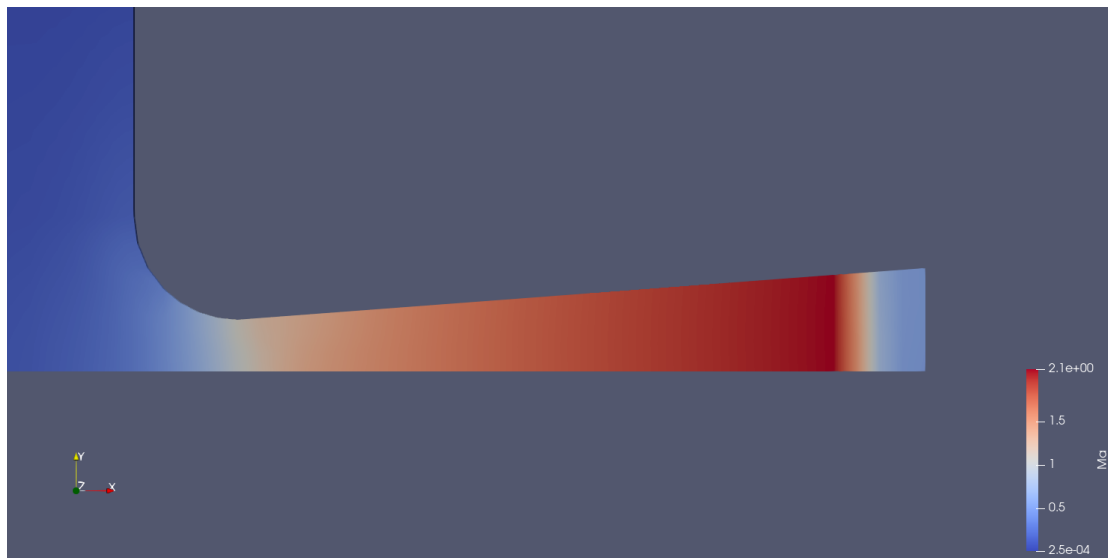


Figure 3.4: Mach number contour for Laval nozzle for supersonic case with a standing normal shock wave at an outlet pressure of 5280 Pa



Figure 3.5: Pressure contour for Laval nozzle for supersonic case with a standing normal shock wave at an outlet pressure of 5280 Pa

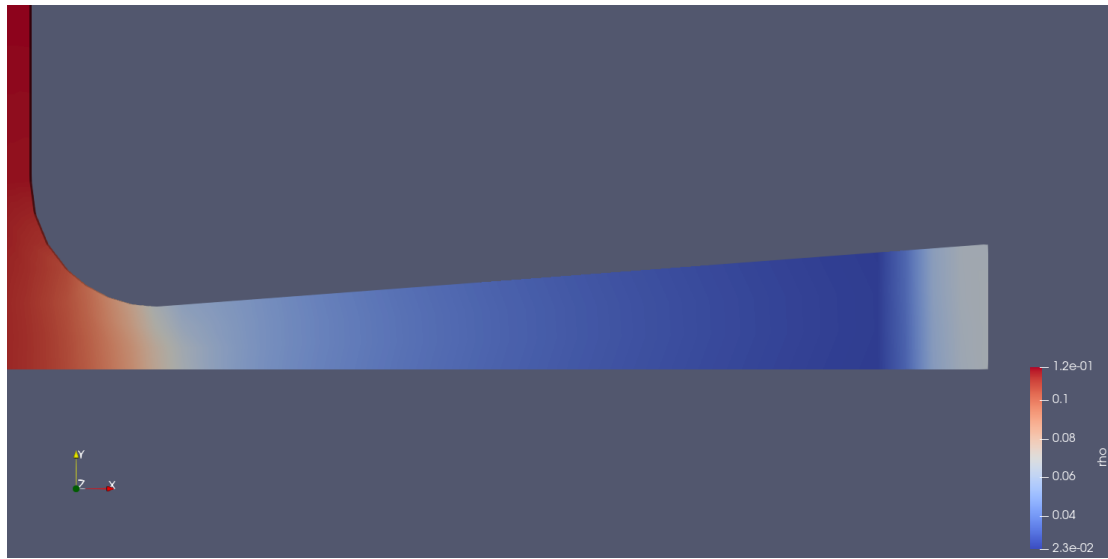


Figure 3.6: Density contour for Laval nozzle for supersonic case with a standing normal shock wave at an outlet pressure of 5280 Pa

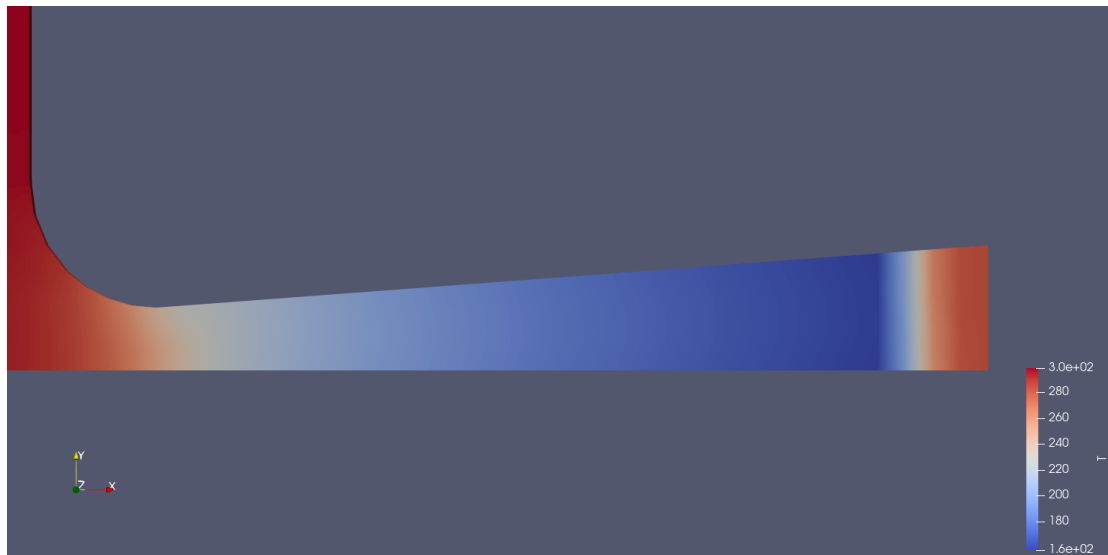


Figure 3.7: Temperature contour for Laval nozzle for supersonic case with a standing normal shock wave at an outlet pressure of 5280 Pa

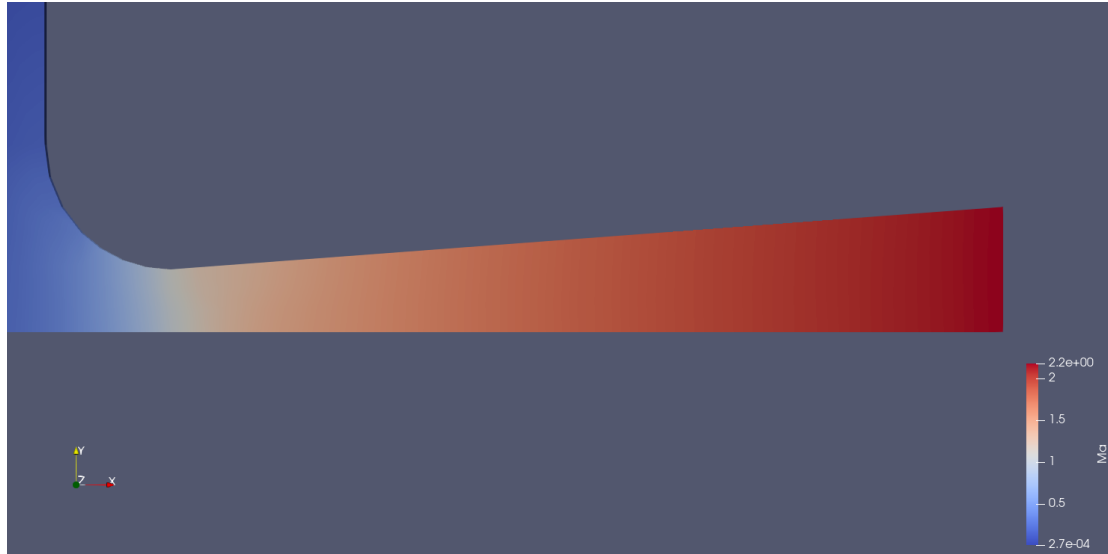


Figure 3.8: Mach number contour for Laval nozzle for supersonic case without shocks at an outlet pressure of 939 Pa



Figure 3.9: Pressure contour for Laval nozzle for supersonic case without shocks at an outlet pressure of 939 Pa

3.2.3 Supersonic case

Analytically it was proved that at outlet pressure of 939 Pa the flow will have exit mach number above than 1 without any shocks. I this case as seen in Figure 3.8 and Figure 3.9 the mach number first increases as a nozzle in converging section and in the diverging section the flow mach number increases. In this case the shock is not observed since the shock has travelled through the nozzle and finally this case is observed where the shock has been detached from the nozzle but this impacts the nature as large amount of sound is observed in the environment which needs to be managed as it is harmful to mankind but this has definitely made the flow supersonic with just subsonic speed we could observe supersonic exit which in turn gives the object supersonic speeds.

The Figure 3.10 shows the plot of various properties like Area ratio (A/A^*), mach number, velocity, density and temperature along the pressure ratio of exit pressure to inlet pressure and it shows the variation of mach number increasing as the pressure ratio increases. It also shows that velocity also increasing throughout the Laval showing that the effective condition of nozzle is achieved. Also the variation of area ratio along the pressure ratio where the geometry of the nozzle is seen and at throat we could observe the mach reaching unity which helps the flow to

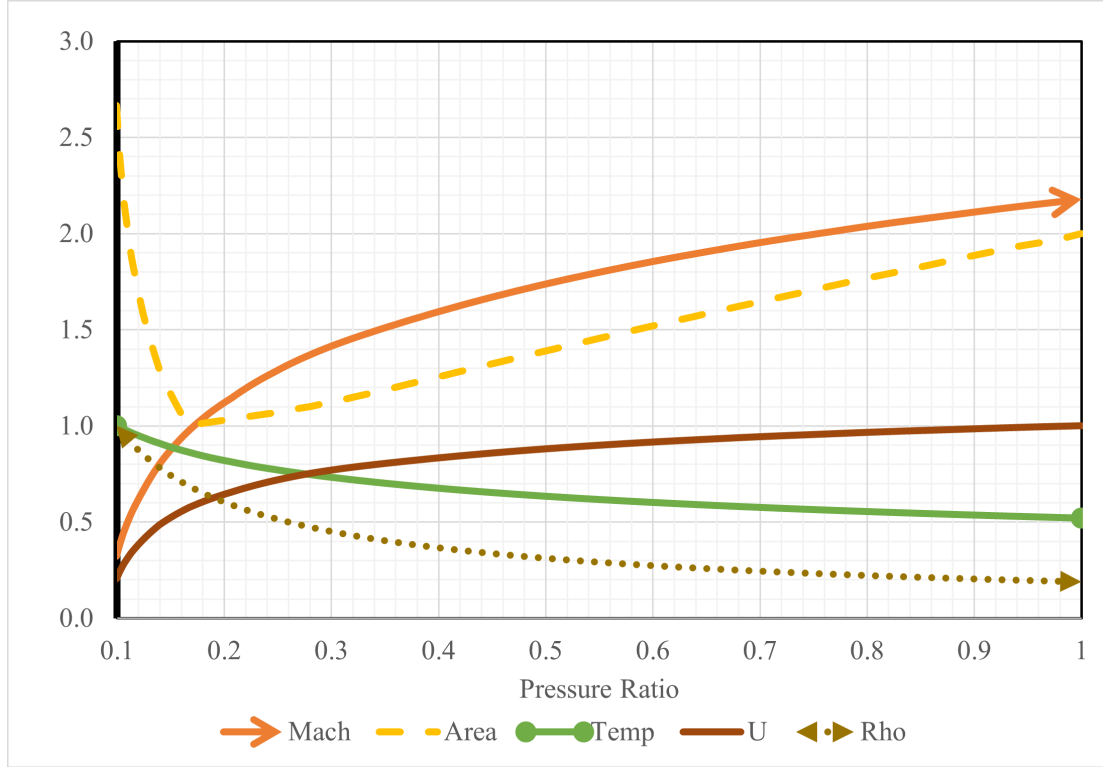


Figure 3.10: Plot depicting the changes in mach number, area ratio, velocity, temperature, and density along the pressure ratio of the Laval nozzle in a supersonic scenario without the presence of any shocks.

Exit pressure [Pa]	Pressure ratio	Exit mach number	Comment
993	0.0993	2.1784	Supersonic flow
5280	0.5703	0.5118	Normal shock observed
6000	0.6480	0.4525	Normal shock observed
7250	0.7813	0.3811	Normal shock observed
8500	0.9160	0.3341	Normal shock observed
9371	0.9855	0.2928	Subsonic flow

Table 3.2: Pressure variation cases for different outlet pressures and corresponding exit mach number observed with comments

get supersonic flow. Variation of Temperature and density along the pressure ratio keeps on decreasing through the nozzle. This is an perfect example of flow for observing the variations of parameters along the nozzle geometry.

3.2.4 Pressure variation

The entire process of varying the pressure ratio and observing the variation of mach number including presence of shocks the Laval nozzle journey needs to be observed. In this pressure variation is performed along the nozzle for the Laval nozzle from subsonic case to supersonic case at the exit is experienced.

The Figure 3.11 shows different cases in which the outlet pressure is varied and we observe subsonic case at first and as increase the pressure difference we observe supersonic flows but with a shock and later as the shocks keeps on moving forwards there is a case where the flow becomes completely shock free and finally the supersonic exit is observed. The different cases with their exit mach numbers are tabulated in the Table 3.2.

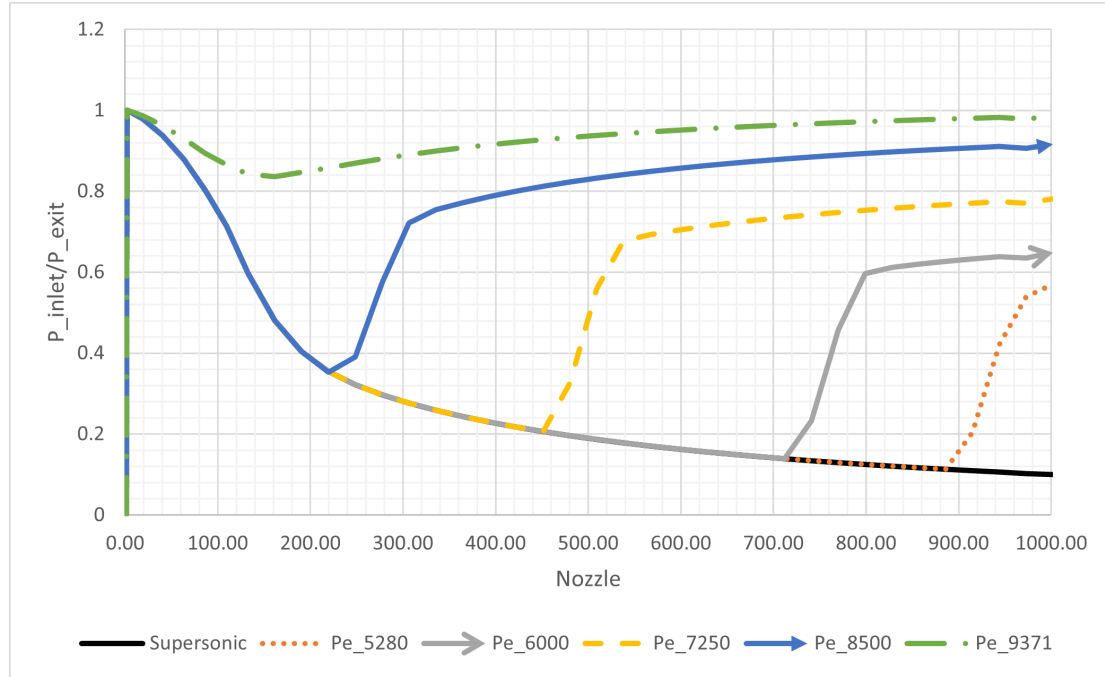


Figure 3.11: Plot of pressure ratio along the nozzle length non-dimensionalized for outlet pressures of 939Pa (supersonic), 5280Pa, 6000Pa, 7250Pa, 8500Pa, 9371Pa for the Laval nozzle

Case	Analytical exit Mach number	CFD exit Mach number	Error (%)
Subsonic case	0.3059	0.2928	4.28
Normal shock case	0.5335	0.5118	4.06
Supersonic case	2.1972	2.1784	0.85

Table 3.3: Comparison of results for exit Mach number with analytical results for subsonic, normal shock, and supersonic cases with error in %

3.2.5 Final Discussion

The simulation performed and the comparison with analytical calculations is important parameter to look towards. The Table 3.3 contains the data for analytical results and simulation results for the 3 cases. Observing the results a comment can be made that for all cases the error percentage is quite less and hence CFD results are in quite agreement with the analytical results.

CONCLUSION

Laval nozzle with rhoCentralFoam solver has been simulated and studied using the OpenFOAM software. The simulation is run for different mesh sizes and also compared to the analytical results and medium mesh is chosen for simulating further studies.

The Laval nozzle problem is also solved for different cases of pressure ratios with a subsonic case, a supersonic case with shock formation and a supersonic case. It is also studied for pressure variation at different pressure ratios and observing the flow move from subsonic case to supersonic case.

The Mach number, pressure ratio, temperature, density, and velocity for the supersonic case are observed along the nozzle geometry and it is observed that the Mach number in the converging section increases until 1 and gets choked exits the nozzle exit at the supersonic Mach number.

Finally, a comparison is made between analytical results and CFD results for exit Mach number and also the error percentage is calculated for 3 different cases of subsonic, supersonic with shock and supersonic case of the Laval nozzle. It was found that the results are in good agreement with analytic solutions.

4.1 Limitations

During the simulation many limitations are found and can be incorporated in further study as well such as

- Understanding the solver rhoCentralFoam and comparing it with other solvers for shock capturing.
- Trying different schemes to decrease the error percentage.
- Adding a domain at the rear end and removing the domain at the front as some amount of flow is lost before the entry to the nozzle.
- Mesh refining to observe good results
- Adding viscosity and also adding boundary layer phenomenon.

REFERENCES

1. J. P. Fernandez and J. Sesterhenn, "Numerical Simulations of a supersonic starting jet at high Reynolds number and its acoustic field," in 20th International Congress on Sound and Vibration 2013, ICSV 2013, 2013, pp. 3.
2. K. Yadav, D. Daware, V. Akolkar, and P. Padalwar, "A Study on Concepts De-Laval Nozzle using CFD Tool," Graduate Research in Engineering and Technology (GRET), vol. 1, no. 7, 2022, Article 17, DOI: 10.47893/GRET.2022.1132.
3. K. Srathonghuam, A. Boonpan, and J. Thongsri, "CFD Simulation of gas flow in a 122 mm supersonic nozzle," in 2022 37th International Technical Conference on Circuits/Systems, Computers and Communications (ITC-CSCC), Phuket, Thailand, 2022, pp. 1-4, DOI: 10.1109/ITC-CSCC55581.2022.9894927.
4. N. D. Deshpande, S. S. Vidwans et al., "Theoretical and CFD Analysis Of De Laval Nozzle," International Journal of Mechanical And Production Engineering, vol. 2, no. 4, April 2014, ISSN: 2320-2092.
5. A. Kurganov and E. Tadmor, "New High-Resolution Central Schemes for Nonlinear Conservation Laws and Convection–Diffusion Equations," Journal of Computational Physics, vol. 160, no. 1, 2000, pp. 241–282, DOI: <https://doi.org/10.1006/jcph.2000.6459>.

APPENDICES

APPENDIX A

The following are the code used for CFD of Laval nozzle using OpenFOAM.

A.1 BlockMeshDict

```

/*-----*- C++ -*-----*\
| =====|
|  \ \ /  F i e l d      | OpenFOAM: The Open Source CFD Toolbox |
|  \ \ /  O p e r a t i o n | Version:  v2306                    |
|  \ \ /  A n d             | Website:  www.openfoam.com          |
|  \ \ /  M a n i p u l a t i o n |                               |
\*-----*-*/

FoamFile
{
    version      2.0;
    format       ascii;
    class        dictionary;
    object       blockMeshDict;
}

// * * * * *

scale 0.1;

vertices
(
    (-0.6 0 -0.005)          // 0
    (-0.2121321 0 -0.005)    // 1
    (0 0 -0.005)             // 2
    (2 0 -0.005)             // 3
    (-0.6 0.45 -0.005)       // 4
    (-0.3 0.45 -0.005)       // 5
    (0 0.15 -0.005)          // 6
    (2 0.3 -0.005)           // 7
    (-0.6 0 0.005)           // 8
    (-0.2121321 0 0.005)     // 9
    (0 0 0.005)              // 10
    (2 0 0.005)              // 11
    (-0.6 0.45 0.005)        // 12
    (-0.3 0.45 0.005)        // 13
    (0 0.15 0.005)           // 14
    (2 0.3 0.005)            // 15

```

```

(-0.2121321 0.237867965 -0.005) // 16
(-0.2121321 0.237867965 0.005) // 17
(-0.6 0.237867965 -0.005) // 18
(-0.6 0.237867965 0.005) // 19
(-4 0 -0.005) // 20
(-4 0.237867965 -0.005) // 21
(-4 0.45 -0.005) // 22
(-4 3.85 -0.005) // 23
(-0.6 3.85 -0.005) // 24
(-0.3 3.85 -0.005) // 25
(-4 0 0.005) // 26
(-4 0.237867965 0.005) // 27
(-4 0.45 0.005) // 28
(-4 3.85 0.005) // 29
(-0.6 3.85 0.005) // 30
(-0.3 3.85 0.005) // 31
);

blocks
(
  hex (9 8 19 17 1 0 18 16) (8 3 1) simpleGrading (1 1 1)
  hex (17 19 12 13 16 18 4 5) (8 3 1) simpleGrading (1 1 1)
  hex (10 9 17 14 2 1 16 6) (4 3 1) simpleGrading (1 1 1)
  hex (11 10 14 15 3 2 6 7) (30 3 1) simpleGrading (1 1 1)
  hex (8 26 27 19 0 20 21 18) (23 3 1) simpleGrading (1 1 1)
  hex (19 27 28 12 18 21 22 4) (23 3 1) simpleGrading (1 1 1)
  hex (12 28 29 30 4 22 23 24) (23 10 1) simpleGrading (1 1 1)
  hex (13 12 30 31 5 4 24 25) (8 10 1) simpleGrading (1 1 1)
);

edges
(
  arc 5 16 (-0.295442325 0.397905546 -0.005)
  arc 16 6 (-0.052094453 0.154557674 -0.005)
  arc 13 17 (-0.295442325 0.397905546 0.005)
  arc 17 14 (-0.052094453 0.154557674 0.005)
);

boundary
(
  inlet1
  {
    type patch;
    faces
    (
      (20 26 27 21)
      (21 27 28 22)
      (22 28 29 23)
    );
  }
  top
  {
    type wall;
    faces
    (
      (23 29 30 24)
      (24 30 31 25)
    );
  }
);

```

```

    );
}
outlet
{
    type patch;
    faces
    (
        (11 3 7 15)
    );
}
bottom
{
    type symmetryPlane;
    faces
    (
        (8 0 1 9)
        (9 1 2 10)
        (10 2 3 11)
        (26 20 0 8)
    );
}
nozzle
{
    type wall;
    faces
    (
        (5 13 17 16)
        (16 17 14 6)
        (6 14 15 7)
        (13 5 25 31)
    );
}
);

mergePatchPairs
(
);

// ***** //

```

A.2 Pressure

```

/*-----*- C++ -*-----*\
| =====|
| \ \ / F i e l d | OpenFOAM: The Open Source CFD Toolbox |
| \ \ / O p e r a t i o n | Version: v2306 |
| \ \ / A n d | Website: www.openfoam.com |
| \ \ / M a n i p u l a t i o n |
| \ \ / |
\*-----*/
FoamFile
{
    version      2.0;
    format       ascii;
    class        volScalarField;
    object       p;
}
// * * * * *

dimensions      [1 -1 -2 0 0 0 0];

internalField    uniform 10000;

boundaryField
{
    inlet1
    {
        type totalPressure;
        p0 uniform 10000;
        gamma 1.4;
        value $internalField;
    }
    outlet
    {
        type fixedValue;
        value uniform 5280;
    }
    bottom
    {
        type symmetryPlane;
    }
    top
    {
        type zeroGradient;
    }
    nozzle
    {
        type zeroGradient;
    }
    defaultFaces
    {
        type empty;
    }
}

// *****

```

A.3 Temperature

```

/*-----*- C++ -*-----*\
| =====|
| \ \ / F i e l d | OpenFOAM: The Open Source CFD Toolbox|
| \ \ / O p e r a t i o n | Version: v2306 |
| \ \ / A n d | Website: www.openfoam.com |
| \ \ / M a n i p u l a t i o n | |
\*-----*/
FoamFile
{
    version      2.0;
    format       ascii;
    class        volScalarField;
    object       T;
}
// * * * * * //

dimensions      [0 0 0 1 0 0 0];

internalField   uniform 298;

boundaryField
{
    inlet1
    {
        type fixedValue;
        value uniform 298;
    }
    outlet
    {
        type zeroGradient;
    }
    top
    {
        type slip;
    }
    bottom
    {
        type symmetryPlane;
    }
    nozzle
    {
        type zeroGradient;
    }
    defaultFaces
    {
        type empty;
    }
}

// * * * * * //

```


A.4 Velocity

```

/*-----*- C++ -*-----*\
| =====|
| \\      / F ield      | OpenFOAM: The Open Source CFD Toolbox|
| \\      / O peration  | Version:  v2306                      |
| \\      / A nd        | Website:  www.openfoam.com            |
| \\      / M anipulation|                                     |
\*-----*-*/
FoamFile
{
    version      2.0;
    format       ascii;
    class        volVectorField;
    object       U;
}
// *****

dimensions      [0 1 -1 0 0 0 0];

internalField    uniform (0 0 0);

boundaryField
{
    inlet1
    {
        type zeroGradient;
    }
    outlet
    {
        type zeroGradient;
    }
    bottom
    {
        type symmetryPlane;
    }
    top
    {
        type slip;
    }
    nozzle
    {
        type slip;
    }
    defaultFaces
    {
        type empty;
    }
}

// *****

```

A.5 FVSolution

```

/*-----*- C++ -*-----*\
|=====|
|  \ \   /  F i e l d      | OpenFOAM: The Open Source CFD Toolbox |
|  \ \   /  O peration     | Version:  v2306                      |
|  \ \   /  A nd           | Website:  www.openfoam.com            |
|  \ \   /  M anipulation  |                                     |
\*-----*/
FoamFile
{
    version      2.0;
    format       ascii;
    class        dictionary;
    object       fvSolution;
}
// * * * * *

solvers
{
    "(rho|rhoU|rhoE)"
    {
        solver      diagonal;
    }

    U
    {
        solver      smoothSolver;
        smoother     GaussSeidel;
        nSweeps      2;
        tolerance    1e-09;
        relTol       0.01;
    }

    e
    {
        $U;
        tolerance    1e-10;
        relTol       0;
    }
}
// *****

```

A.6 FVSchemes

```

/*-----*- C++ -*-----*\
| =====|
| \\      / F ield      | OpenFOAM: The Open Source CFD Toolbox |
| \\      / O peration  | Version:  v2306                      |
| \\      / A nd        | Website:  www.openfoam.com            |
| \\      / M anipulation|                                     |
\*-----*-*/
FoamFile
{
    version      2.0;
    format       ascii;
    class        dictionary;
    object       fvSchemes;
}
// * * * * *

fluxScheme      Kurganov;

ddtSchemes
{
    default      Euler;
}

gradSchemes
{
    default      Gauss linear;
}

divSchemes
{
    default      none;

    div(tauMC)   Gauss linear;
}

laplacianSchemes
{
    default      Gauss linear corrected;
}

interpolationSchemes
{
    default linear;
    reconstruct(rho) vanAlbada;
    reconstruct(U)  vanAlbadaV;
    reconstruct(T)  vanAlbada;
}

snGradSchemes
{
    default      corrected;
}

```

// ***** //

A.7 ControlDict

```

/*-----*- C++ -*-----*\
| =====|
| \\ / F ield | OpenFOAM: The Open Source CFD Toolbox |
| \\ / O peration | Version: v2306 |
| \\ / A nd | Website: www.openfoam.com |
| \\ M anipulation |
\*-----*/
FoamFile
{
    version      2.0;
    format       ascii;
    class        dictionary;
    object       controlDict;
}
// * * * * *

application     rhoCentralFoam;

startFrom        latestTime;

startTime        0;

stopAt           endTime;

endTime          2;

deltaT           0.00001;

writeControl     adjustableRunTime;

writeInterval    0.1;

purgeWrite       0;

writeFormat      ascii;

writePrecision   6;

writeCompression off;

timeFormat       general;

timePrecision    6;

runTimeModifiable true;

adjustTimeStep   yes;

maxCo            0.25;

maxDeltaT        1;

functions
{

```

```
libs          (fieldFunctionObjects);

Ma
{
    type      MachNo;
    executeControl writeTime;
    writeControl writeTime;
}

// ***** //
```

A.8 Turbulence Properties

```

/*-----*- C++ -*-----*\
| =====|
| \\      / F ield      | OpenFOAM: The Open Source CFD Toolbox|
| \\      / O peration  | Version:  v2306                      |
| \\      / A nd        | Website:  www.openfoam.com           |
|  \\\\    M anipulation |                                     |
\*-----*/
FoamFile
{
    version      2.0;
    format       ascii;
    class        dictionary;
    object       turbulenceProperties;
}
// * * * * *

simulationType  laminar;

// *****

```

A.9 Thermal Properties

```

/*-----*- C++ -*-----*\
| ===== |
| \\      / F ield      | OpenFOAM: The Open Source CFD Toolbox|
| \\      / O peration  | Version: v2306                      |
| \\      / A nd        | Website: www.openfoam.com           |
|  \\     / M anipulation |
\*-----*/
FoamFile
{
    version      2.0;
    format       ascii;
    class        dictionary;
    object       thermophysicalProperties;
}
// * * * * * //
thermoType
{
    type          hePsiThermo;
    mixture        pureMixture;
    transport      const;
    thermo         hConst;
    equationOfState perfectGas;
    specie         specie;
    energy         sensibleInternalEnergy;
}
mixture
{
    specie
    {
        nMoles      1;
        molWeight    29;
    }
    thermodynamics
    {
        Cp          1005;
        Hf          0;
    }
    transport
    {
        mu          0;
        Pr          1;
    }
}
// ***** //

```